Pervasive and Mobile Computing 8 (2012) 68–81

Contents lists available at SciVerse ScienceDirect

Pervasive and Mobile Computing

journal homepage: www.elsevier.com/locate/pmc

Fast track article

# Swimming performance and technique evaluation with wearable acceleration sensors

Marc Bächlin *, Gerhard Tröster

*Wearable Computing Laboratory, ETH Zürich, Switzerland*

ARTICLE INFO

*Article history:*
Received 28 December 2009
Received in revised form 18 April 2011
Accepted 17 May 2011
Available online 25 May 2011

*Keywords:*
Swimming
Wearable system
Context recognition
Performance evaluation
*SwimModel*

ABSTRACT

We are working towards a wearable computing system called *SwimMaster*, that will support swimmers in achieving their desired exercise goals by monitoring their swimming performance and technique and providing the necessary feedback. In this article, we describe our methods to extract the most relevant swimming performance and technique parameters from acceleration sensors worn at the wrist and at the back. We analyze the data and our methods with a *SwimModel*. Finally, we present the results of our evaluation studies with 18 swimmers—seven elite, eight recreational and three occasional swimmers.



## 1. Introduction and motivation

The performance of swimming is strongly related to the swimmer's technique. Therefore, a swimmer who wants to improve his swim performance has to devote a substantial proportion of the training to his swim style improvement. Apart from a swimmer's effort of heading forward efficiently, the swimmer needs to be concerned about breathing and floating at the water surface.

The two most important physical principles to swim faster and more efficiently are:

- Reduction of water resistance through an improved *body balance* and *body rotation*.
- Increasing of the propelling force by improving the arm strokes and hence the *stroke efficiency*.

The consensus nowadays is that both factors must be optimized. The result of an improved streamlined position together with an increased propelling force is *synergetic swimming*, meaning that both factors have to be improved likewise for fast swimming [1].

*Stroke efficiency* is an indication of the swimmer's technique. The parameters to determine the efficiency of the stroke mechanics are the stroke length, measured as *distance per stroke* (*DPS*) in m/stroke and the swimming speed $v$, measured in m/min. With an improved stroke technique, fewer strokes per distance are needed while swimming at constant speed. On the other hand, a swimmer's technique has improved, if he swims faster with the same number of strokes per distance, e.g. one lane [2].

*Body balance* refers to the angle between the swimmer's body and the water surface. A good body balance is crucial for efficient swimming as drag forces are reduced enormously. There are several possible reasons for a bad body balance in crawl swimming, for example, weak leg kicks, a weak body tension or a bad posture of the head due to looking upwards instead of aligning spine and head.

* Corresponding author.
*E-mail addresses:* baechlin@ife.ee.ethz.ch (M. Bächlin), troester@ife.ee.ethz.ch (G. Tröster).

1574-1192/$ – see front matter © 2011 Elsevier B.V. All rights reserved.
doi:10.1016/j.pmcj.2011.05.003

*Body rotation* refers to the swimmer's body rotation along his longitudinal body axis. Body rotation is efficient in crawl and backstroke swimming because the stroke length can be increased and the side-lying gliding position is the body position with the least water resistance. The body rotation is ideally initiated by the leg kicks. The upper and the lower body part should rotate together, because a synchronized rotation leads to a fluent motion. By contrast, a twist between the upper and lower body results in an inefficient winding swim trajectory.

The strong influence of a good technique in swimming can be seen at national and international swimming competitions, where even 40-, 50- and 60-year old swimmers sometimes achieve their personal best time. Many of these sportsmen have been competitive swimmers in their earlier life when they have been 15–25 years old, some even Olympic participants. This is possible because they have improved their training technique and hence their swimming technique. Although they have less power and are less agile than in their younger days, they swim faster now with the improved technique [1].

Nowadays we know more about the best and most efficient swim techniques than several years ago, but the swimming performance evaluation methods are still the same. There are the three observation methods of (i) self-perception (ii) supervision by the swimming trainer and (iii) video analysis. All three methods have their advantages and disadvantages.

(i) By self-perception, the swimmer "feels the water" and can react to perceived forces. This allows him to react to faults instantly. However, the swimmer must be experienced to be able to identify faults himself.
(ii) On the other side, video analysis is the most objective evaluation method. However, video analysis can only be done off-line, it is time consuming, and the swimmer cannot correct his errors instantly. In addition, underwater cameras are not allowed in public swimming pools to protect the privacy of other swimming pool visitors.
(iii) Direct supervision by a trainer is the most frequently used observation method. The trainer can give direct instructions to the swimmer but he can only observe one swimmer at a time. Observation by the trainer also has its limitations, as movements below the water surface are difficult to observe.

Many recreational swimmers and triathletes often train alone and do not have a trainer aside at all times or access to video analysis. They are non-professional athletes and do not have the necessary experience and sense of self-perception. The *SwimMaster* will help these athletes keep track of their technique in the training hours where no trainer is present. In addition, it can support the trainer during his training hours by providing additional continuous swim performance parameters not available so far.

## 2. Related work

Science and new techniques strongly influence the world of sports nowadays. Especially during the last 10–20 years, many electrical devices have been developed to support the training of an athlete. Most well known wearable sport computers nowadays are probably heart rate monitors, widely used in many sports to capture and display the heart rate of the sportsman, e.g. the Polar RS400[1] or the Suunto t6c.[2] Pervasive computing has further successfully been applied to different areas in the world of sport in disciplines like cycling[3] or diving.[4] Further, there is pervasive computing applied to sports like running [3], skiing [4], snowboard [5,6], ski-jumping [7], golf [8,9], rowing [10], football games [11,12], baseball [13], and table tennis [14].

The typical wearable sport device is wrist worn, equipped with tiny buttons on the side or on the top, features a small liquid crystal display, and a piezo-electric beeper. Besides a sensor unit to capture e.g. speed, distance, depth or heart rate, all these products provide the user with information about his current performance and/or physical state.

For swimmers there are only a few commercial swim-timer devices available, which can be used to measure lane times and to count the number of lanes swum. There are devices to be placed on the pool wall, e.g. the *Lap Track*,[5] or worn on the swimmers finger, e.g. *SportCount Chrono* 100.[6] They are based on push buttons and a display.

Current research on mobile, body worn systems focuses on context and activity awareness. Applied to swimming, a context aware computing system can relieve the swimmer from e.g. manually pressing a button to count the lanes and stop the time.[7]

Ohgi analyzed the stroke phases of a wrist worn motion sensor to quantify the swimmer's fatigue [15]. Davey et al. used a sensor on the swimmer's hip to extract the strokes of front crawl swimming [16,17]. Chan has patented a method using a magnetic field sensor to count the number of lanes swum [18]. Discriminating the four competition swim styles by accelerometer sensors has been investigated by Slawson et al. [19].

All these previous works show the potential of body worn sensors in swimming as it has been summarized by Callaway et al. [20]. However, previous work just presented methods to extract single parameters of swimming such as e.g. the

1 Polar electro Europe bv. http://www.polar.fi/en/, December 2009.
2 Suunto Finland. http://www.suunto.com, December 2009.
3 Ciclosport. http://www.ciclosport.de, December 2009.
4 Mares http://www.mares.com, December 2009.
5 Finis inc. http://www.finisinc.com, December 2009.
6 Sportcount http://www.sportcount.com, December 2009.
7 Pool-Mate http://www.swimovate.com/, December 2009.

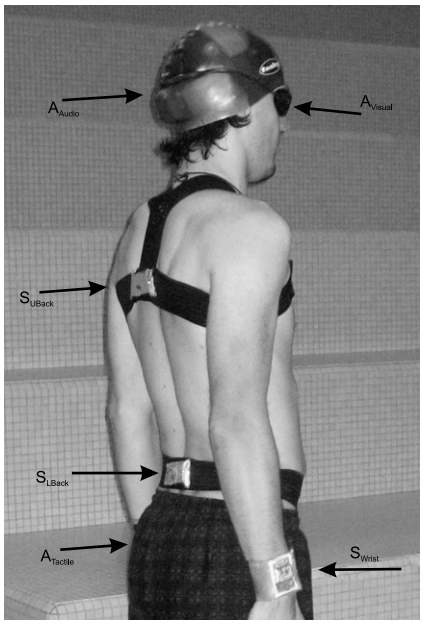


**Fig. 1.** Picture showing the sensors ($S_x$) and actuators ($A_x$) mounting positions.

arm strokes, the lap counts or the swim style. None of them has worked on the overall goal of stroke efficiency and swim technique evaluation. We have been the first proposing a wearable system to perform an automatic stroke efficiency evaluation [21]. Furthermore we introduced the *SwimMaster* system [22] and developed a *SwimModel* to simulate the sensor signal recorded during swimming [23]. In this work we combine both works, the wearable *SwimMaster* system and the *SwimModel*. We show how the *SwimModel* is used to evaluate the body-balance and body-rotation measurements of the wearable *SwimMaster* system.

## 3. The *SwimMaster* system

We built a *SwimMaster* prototype system as depicted in Fig. 1. The *SwimMaster* hardware consists of two major building blocks, namely the *SwimRecorder* for motion measurement and recording and the *Swim-Feedback-System* for user feedback [22]. Four sensors are mounted at the swimmer's upper and lower back ($S_{UBack}$, $S_{LBack}$) and at the left and right wrist ($S_{LWrist}$, $S_{RWrist}$). Furthermore the subject depicted in Fig. 1 wears the visual feedback swim goggles ($A_{Visual}$), the tactile ($A_{Tactile}$) and the acoustic ($A_{Audio}$) feedback devices. The data read from the acceleration sensor is not yet processed online at this early stage but is stored for off-line processing. True online feedback is therefore not yet possible with this system.

In the next section we describe the *SwimRecorder* system we used for the data recording and evaluation of our parameter extraction methods. Details on the *Swim-Feedback-System* are described in [24].

### 3.1. The SwimRecorder

For the data acquisition of our swim studies we developed a *SwimRecorder* [22]. The *SwimRecorder* consists of a 3-axes accelerometer sensor, a micro-controller, 1 GB of flash memory and a rechargeable battery. The acceleration signals are converted by a 10 Bit A/D converter and sampled at a frequency of 256 Hz. With the 3.7 V, 250 mAh battery pack continuous data recording of up to 48 h is possible. With a weight of 34 g and the dimensions of $36 \times 42 \times 12$ mm$^3$ the device can unobtrusively be worn by the swimmer without hindering him while swimming. Watertightness is ensured by shrink-wrapping the device in plastic foil. The device is started and stopped over a contactless reed switch.

The fixation of the wrist sensors $S_{LWrist}$ and $S_{RWrist}$ is like a wristwatch. The sensor is put in a transparent plastic tube, which is fixed at the swimmer's wrist using velcro fasteners. The orientation of the acceleration sensor as well as the packaging and fixation of the *SwimRecorder* is shown in Fig. 2. The lower back sensor $S_{LBack}$ is mounted on the hip with an elastic stretch band, worn like a belt. Velcro fasteners help to fit the band to the swimmer's body. The upper back sensor $S_{UBack}$ is mounted between the shoulders with elastic bands combined to a harness. The fixation ensures that the sensors do not shift or slip away, but are still comfortable to wear for the swimmer and do not bother him during his swimming exercises. A picture of a swimmer with the sensors attached is shown in Fig. 1. $S_{LBack}$ and $S_{UBack}$ are oriented according to the body coordinate system shown in Fig. 3.

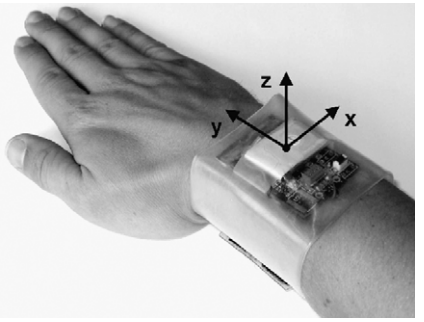


**Fig. 2.** Packaging and fixation of the *SwimRecorder* attached to the swimmer's wrist. The arrows indicate the orientation of the three axes of the acceleration sensor.

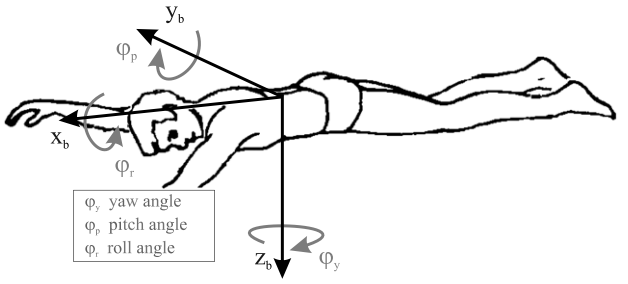


**Fig. 3.** Body coordinate system: orientation and nomenclature of the axis and angles.

### 3.2. Body position and orientation

In the following, we differentiate between two coordinate systems, namely the fixed world coordinate system and the body coordinate system. The linear variables in the world coordinates have a $w$ index; coordinates in body coordinates have a $b$ index. Angular variables do not have an index because they always describe the orientation of the body coordinate system relative to the fixed world coordinate system.

A rigid body has six degrees of freedom, three for the linear position of the center of gravity and three for the orientation. For our description of the swimmer's movement we describe the swimmer's upper body and assume that it is rigid, which is a reasonable assumption for the main upper body where the sensor $S_{UBack}$ is attached.

There are several methods to describe the orientation. We use the *Euler angles*, which describe the body orientation by the three angles $\varphi_y$, $\varphi_p$, $\varphi_r$.[8] Applied to a swimmer, the *Euler angles* are defined in the following order:

1. Rotation around the $Z$-axis by $\varphi_y$, the yaw angle.
2. Rotation around the $Y$-axis by $\varphi_p$, the pitch angle.
3. Rotation around the $X$-axis by $\varphi_r$, the roll angle.

All rotations are right-handed and executed around the body's coordinate axes as depicted in Fig. 3.

The yaw angle $\varphi_y$ is the swim direction. The pitch angle $\varphi_p$ is a measure for the *body balance*. The roll angle $\varphi_r$ describes the *body rotation* around the body's longitudinal axis. In the following the Euler angles $\varphi_y$, $\varphi_p$, $\varphi_r$ are combined to the orientation angle vector $\vec{\varphi} = [\varphi_y\ \varphi_p\ \varphi_r]$.

## 4. *SwimModel* and parameter extraction methods

In this section, we describe our swim parameter extraction methods to measure the swim performance and the swim technique. Furthermore, we explain our *SwimModel*, used to analyze the acceleration signals and to evaluate the accuracy of the body rotation and body balance measurement.

### 4.1. Parameter extraction from the wrist sensors

Within the recorded signal of the wrist sensors we detect the wall-push-off, the wall-turns and the wall-strike events. This detection is based on the gradient of the $y$-axis of $S_{XWrist}$. The raw acceleration signal $a_y$ is low-pass filtered using a second order Butterworth filter with a normalized cutoff frequency of 0.01 to eliminate sensor noise. From the filtered signal $a_{filt}$, the gradient is calculated with a sliding window of 0.2 s.

[8] The *Euler angles* are often called $\alpha$, $\beta$, $\gamma$. We have chosen the $\varphi_y$, $\varphi_p$, $\varphi_r$ nomenclature in order to avoid confusion with the angular acceleration $\vec{\alpha}$.

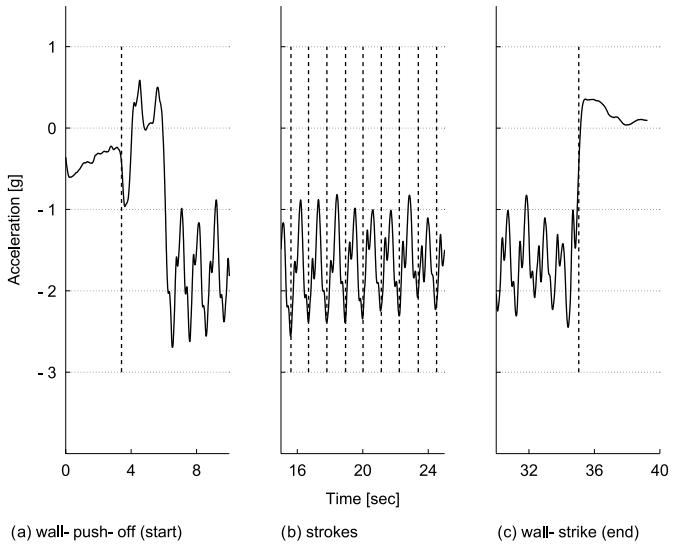


**Fig. 4.** Example of the detected wall-push-off (a), strokes (b) and wall-strike (c) events (line: filtered $y$-axis signal, dashed: detected events).

#### 4.1.1. Swimming velocity

The wall-push-off event is identified by the first falling slope in $a_{filt}$. This falling slope is detected by the first minimum in the gradient as depicted in Fig. 4(a). The wall-strike at the end of the pool is detected by a strongly increasing slope as depicted in Fig. 4(c). This increasing slope is detected by searching for the maximum in the gradient signal.

To determine the average swimming velocity $\bar{v}$ of one lane, the time $t_{lane} = t_{WallStrike} - t_{WallPushOff}$ for the given pool length $d_{lane}$ is measured and the average velocity per lane is calculated by $\bar{v} = \frac{d_{lane}}{t_{lane}}$.

#### 4.1.2. Arm stroke parameters

To detect single arm stokes, a peak detection is applied to $a_{filt}$. In Fig. 4(b) all detected strokes are marked with dashed vertical lines. With the timestamps of all stroke events, the time per stroke ($TPS$) is calculated by $TPS = \frac{T_N - T_1}{N-1}$ with $T_N - T_1$ the time between the first and last stroke and $N$ the number of strokes.

With the average velocity $\bar{v}$ and the average $TPS$, the average distance per stroke ($DPS$) is calculated by the product of both, $DPS = \bar{v} \cdot TPS$.

### 4.2. Parameter extraction from the body sensors

From the body sensor signal, we are not only interested in time events. This is different compared to the parameter extraction from the wrist sensors. Therefore, a detailed understanding of this signal is required. To get a complete understanding of the measured body acceleration we built a *SwimModel*, which describes the relation between measured sensor acceleration signal and input forces, input moments, and swimmer's orientation.

#### 4.2.1. The SwimModel

The *SwimModel* consists of a body motion model based on classical mechanics. Fig. 5 shows the block diagram of the *SwimModel*. The model inputs are the body torques $\vec{M}_{in}$, the arm force $\vec{F}_{arm}$, the leg force $\vec{F}_{leg}$ and the gravity force $\vec{F}_{grav}$. The three input forces together are called input force $\vec{F}_{in}$. Based on $\vec{F}_{in}$ and $\vec{M}_{in}$ the model calculates the swimmer's acceleration $\vec{a}_w$, velocity $\vec{v}_w$ and position $\vec{s}_w$ as well as the angular accelerations $\vec{\alpha}$, angular velocities $\vec{\omega}$ and angles $\vec{\varphi}$.

Internally, the model considers the buoyancy force $\vec{F}_{buoy}$, the drag forces $\vec{F}_{drag}$ and the drag moments $\vec{M}_{drag}$. The transformation of the body motion into the sensor coordinate system and its sensing modalities is done by a sensor model. The sensor model also calculates the centripetal $\vec{F}_{centripetal}$ and tangential $\vec{F}_{tangential}$ accelerations, which are measured by the sensor due to the displacement of the sensor to the rotation axis and the angular velocity $\vec{\omega}$ respectively the angular acceleration $\vec{\alpha}$. A detailed description of this *SwimModel* is given in [23].

#### 4.2.2. The body acceleration signal

Fig. 6 shows a real signal we recorded during our evaluation studies together with the simulated signal using our *SwimModel*. One can see that the *SwimModel* can very effectively simulate the real sensor signal. The most dominant component in this signal is the sinusoidal part in the $y$-axis. The sinusoidal signal in the $z$-axis is the second most dominant

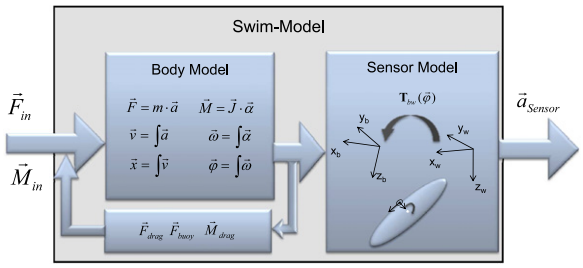


**Fig. 5.** The block diagram of the *SwimModel*.

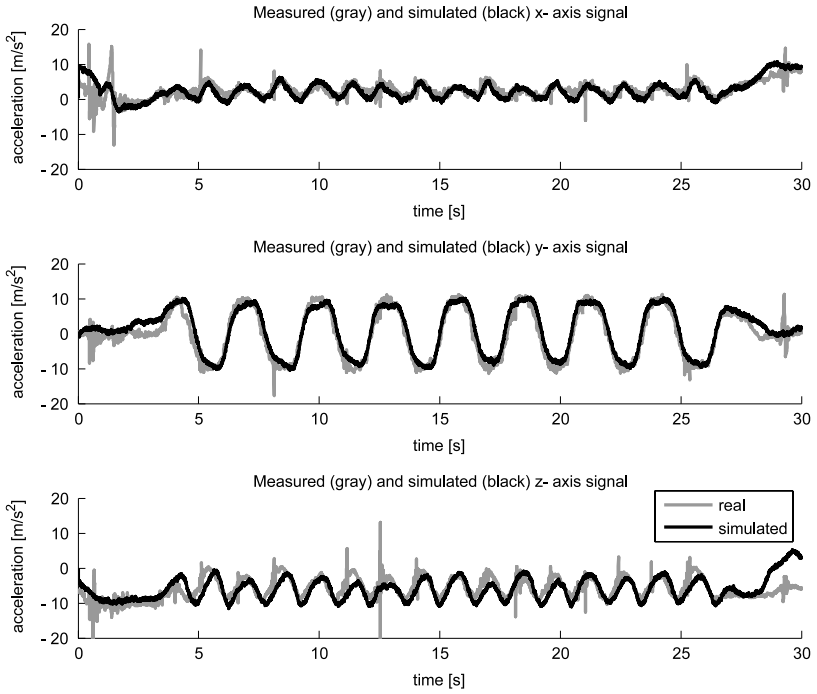


**Fig. 6.** Comparison between a real measured sensor signal (gray) and the simulated sensor signal (black).

part with about half the amplitude of the *y*-axis signal, but twice the frequency. The *x*-axis has the least dominant signal; it is weaker and more irregular.

The simulation allows us to evaluate in detail the different components measured with the acceleration sensor at the back of a swimmer. In the following we analyze and discuss the sensor signal split into the five component parts $\vec{a}_{gravity}$, $\vec{a}_{swim}$, $\vec{a}_{centripetal}$, $\vec{a}_{tangential}$ and $\vec{a}_{noise}$.

$\vec{a}_{gravity}$ is the component due to the gravity and the swimmer's orientation. In the world coordinate system, the gravity $g = 9.81\ \mathrm{m/s^2}$ is given as $\vec{a}_{w\_gravity} = [0 \quad 0 \quad 9.81]$, with only one constant component in the *z*-direction. Due to the changing body orientation while swimming, the sensor measures components of this gravity in all three axes.

$\vec{a}_{swim}$ is the component of the acceleration and deceleration of the swimmer due to the propelling arm and leg forces as well as the drag forces.

$\vec{a}_{centripetal}$ is the centripetal acceleration component due to the sensor displacement to the rotation axes and the angular velocity $\vec{\omega}$.

$\vec{a}_{tangential}$ is the tangential acceleration component due to the sensor placement and the angular acceleration $\vec{\alpha}$.

$\vec{a}_{noise}$ is the simulated sensor noise.

In the following, we explain the influence of these five components on the resulting acceleration. First we run the swimming simulation for an ideal swimmer, which has a constant input force $\vec{F}_{in}$, a constant body balance $\varphi_p$ and a regular sinusoidal body rotation $\varphi_r$. In Fig. 7, one can see that for such an ideal swimmer the sensor would measure a constant acceleration signal on the *x*-axis, a sinusoidal signal on the *y*-axis and a second sinusoidal signal with twice the frequency of the *y*-axis on the *z*-axis (see $\vec{a}_{cen\text{-}tan\text{-}noise}$ in Fig. 7). The frequency of the signal in the *y*-axis is the same as the frequency of the body rotation, respectively the frequency of the arm strokes. Due to the constant input force $\vec{F}_{in}$, there is no signal

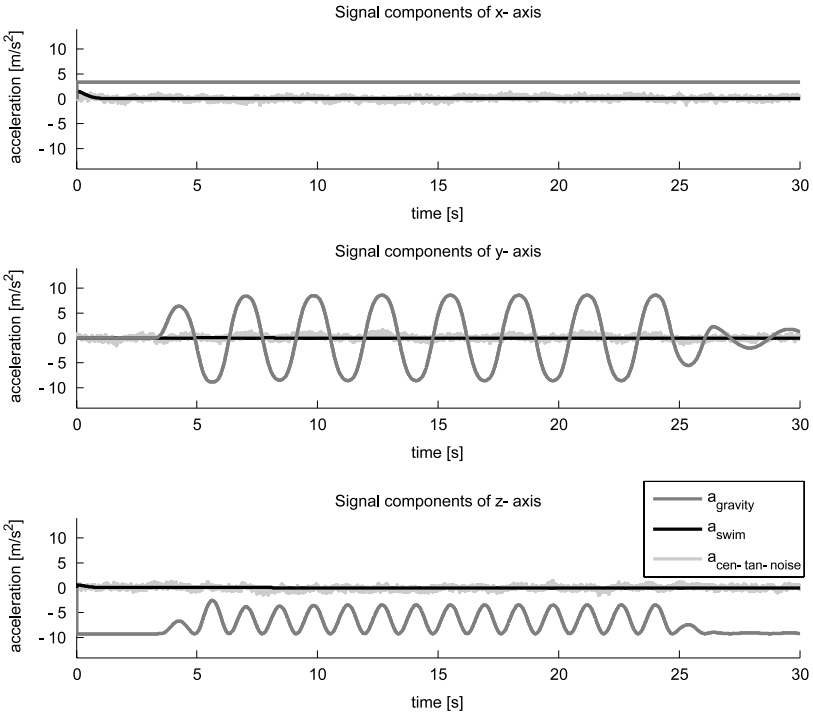


**Fig. 7.** Simulation of the acceleration components, which would be measured if the swimmer swims with a constant input force $\vec{F}_{in}$ and constant body balance. $a_{gravity}$ is the gravity component; $a_{swim}$ is the swimmer's linear movement component; $a_{cen\text{-}tan\text{-}noise}$ are the centripetal, tangential and noise components (this signal component is $< \pm\, 1\ \mathrm{m/s^2}$ around zero).

component $\vec{a}_{swim}$ of the swimmer's movement. The centripetal $\vec{a}_{centripetal}$ and tangential accelerations $\vec{a}_{tangential}$ are within the range of the noise $\vec{a}_{noise}$ and have no significant influence on any axes.

Second, we run the swim simulation with realistic arm forces. The **arm force** $\vec{F}_{arm}$ produced by the arm strokes is therefore modeled with a trapezoid shape. In our model, we differentiate between four arm stroke phases, which are the catch, the pull, the push, and the gliding stroke phase. The catch stroke phase is the part with rising force. The pull stroke phase is the part with constant maximal force. The push stroke phase is the decreasing force part. The gliding phase is the part where no force is applied by the arms. In Fig. 8 one can see that such an input force results in a rippled signal on the *x*-axis, the other two axes are affected in the order of the noise.

Finally, Fig. 9 shows the split sensor signal for the simulated signal of Fig. 6. Due to the changing pitch angle of the swimmer, there is also a changing gravity component in the *x*-axis. Further, one can see that forward swim acceleration is more irregular. This is due to irregular arm forces.

### *4.2.3. Body balance and body rotation measurement*

For the swimming technique evaluation, we are interested in the body balance and the body rotation. For the static case, the roll angle can be determined from the measured gravity in the body coordinate system by the following equation:

$$\varphi_r = \arctan\left(\frac{y_b}{z_b}\right). \tag{1}$$

The roll angle $\varphi_r$ depends on the *y*- and *z*-axis, which are perpendicular to the swim direction. As we have shown in the previous subsection and Fig. 9, the gravity component in the *y*- and *z*-axis is much bigger compared to the other acceleration components. With the *SwimModel* we analyzed the influence of the disturbing acceleration components on the angle measurement. For this purpose, we simulated the acceleration signal during swimming as shown in Fig. 6. In Fig. 9, we have plotted the gravity component $a_{gravity}$, the swimmer's linear movement component $a_{swim}$, and the centripetal, tangential and noise components $a_{cen\text{-}tan\text{-}noise}$. Based on the simulated sensor signal, we calculate the roll angle. Due to the simulation, we also know exactly the correct roll angle. Fig. 10 shows the comparison between the roll angle ($roll_{measured}$) calculated from the simulated acceleration signal and the correct roll angle ($roll_{correct}$). One can see that the irregular forward movement and the changing pitch angle have no influence on the roll angle measurement. Eq. (1) is also valid for the non-static case of swimming.

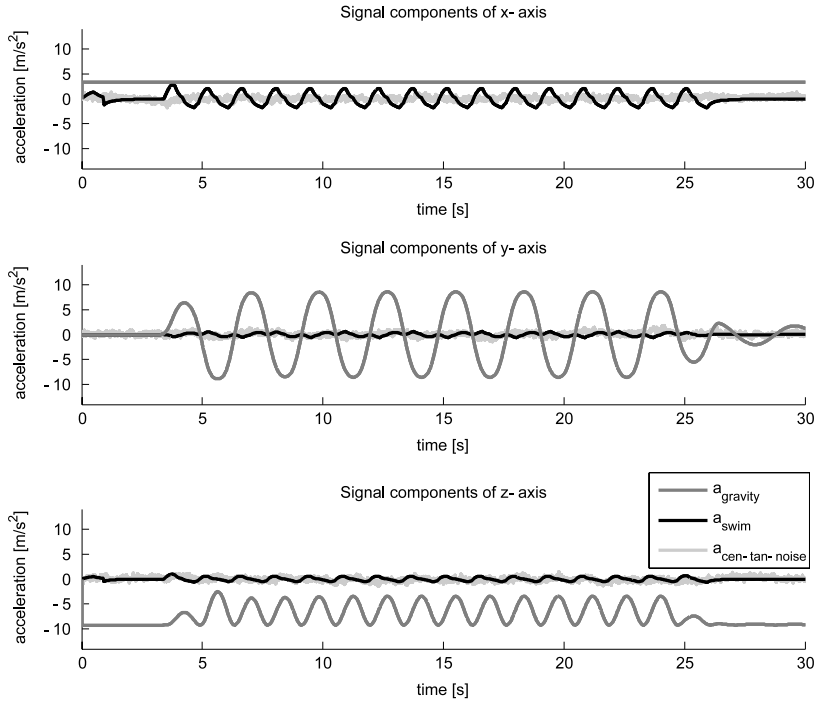


**Fig. 8.** Simulation of the acceleration components, which would be measured if the swimmer swims not with a constant input force $\vec{F}_{in}$ but constant body balance. $a_{gravity}$ is the gravity component; $a_{swim}$ is the swimmers linear movement component; $a_{cen\text{-}tan\text{-}noise}$ are the centripetal, tangential and noise components (this signal component is $< \pm 1\ \mathrm{m/s^2}$ around zero).

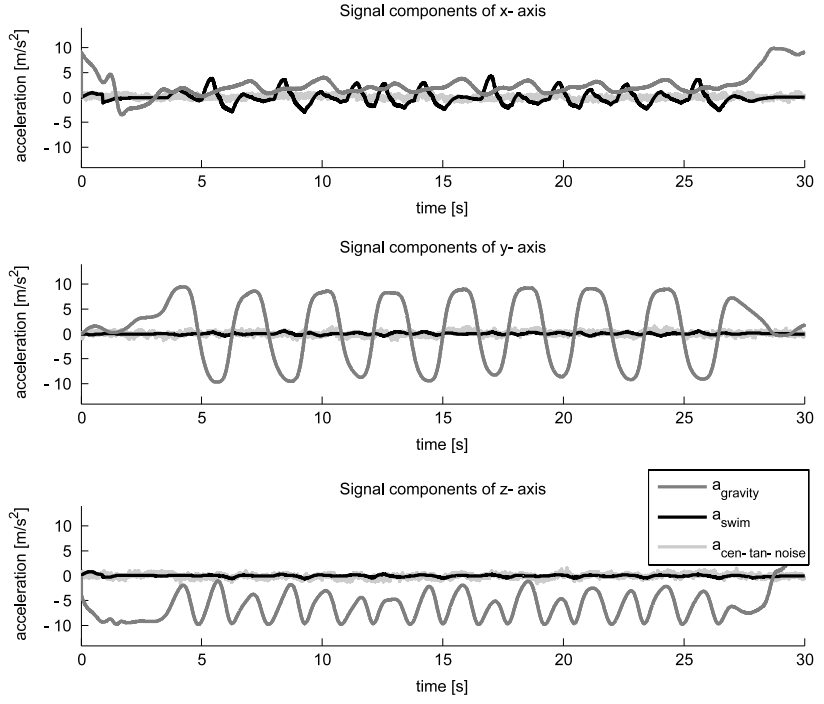


**Fig. 9.** The sensor signal of Fig. 6 split into its component parts. $a_{gravity}$ is the gravity component; $a_{swim}$ is the swimmer's linear movement component; $a_{cen\text{-}tan\text{-}noise}$ are the centripetal, tangential and noise components (this signal component is $< \pm 1\ \mathrm{m/s^2}$ around zero).

Similarly as for the roll angle the pitch angle is given in the static case by the following equation:

$$\varphi_p = -\arcsin\left(\frac{x_b}{9.81}\right). \tag{2}$$

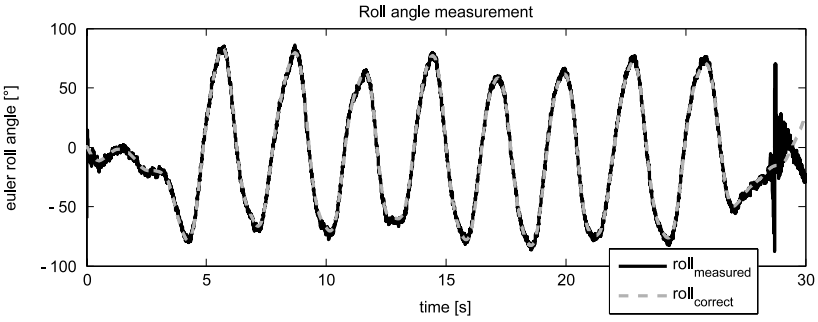


**Fig. 10.** Roll angle measurement: the dashed gray line is the correct roll angle and the black solid line is the measured angle by Eq. (1).

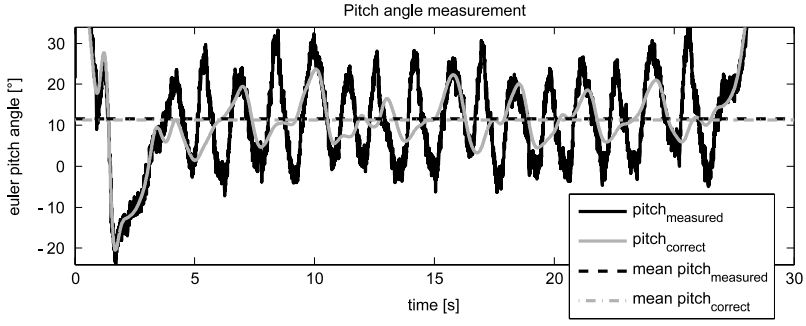


**Fig. 11.** Pitch angle measurement: the black line is the measured pitch angle by Eq. (2) and the gray line is the correct pitch angle. The dashed lines are the average values of the measured and the correct pitch angle.

**Fig. 12.** Video snapshot of a swimmer during our studies.

The body balance angle depends on the forward $x$-axis. This axis is strongly influenced by the irregular forward movement, as one can see in Fig. 9. This results in a bad signal to noise ratio. Similar to the calculation of the roll angle, we calculated the body balance. The pitch angle ($pitch_{measured}$) calculated from the simulated acceleration signal and the correct pitch angle ($pitch_{correct}$) are plotted in Fig. 11. One can see that the body balance can not be calculated correctly from the acceleration signal, due to the bad signal to noise ratio. Therefore it is not possible to calculate the instantaneous pitch angle from the measured acceleration signal, as it is possible for the roll angle. Nevertheless, the average pitch angle ($mean\ pitch_{measured}$) corresponds to the average correct pitch angle ($mean\ pitch_{correct}$), as shown in Fig. 11. Therefore, only the average pitch angle can be calculated from the acceleration sensor signal.

## 5. Swim studies and results

We recorded swimmers' data using the *SwimRecorder* devices mounted to the swimmer as shown in Fig. 1. Swimmers with different level of swimming experience took part in our experiments. We distinguish between three swimmer categories depending on their swimming level. The categories with their names, their explanation, and the numbers of participants are listed in Table 1. Overall, 18 swimmers have taken part in our studies, however not every subject participated in each study. Fig. 12 shows one swimmer in action.

All subjects found our *SwimMaster* prototype rather comfortable to wear and reported that they did not feel restricted in their movements. We do not have objective measures of the imposed drag forces by the system, but subjective feedback from the swimmer reported no noticeable additional water resistance or disturbed fluid dynamics.

**Table 1**
Category names, explanation and number of subjects of the three swimmer groups.

| Category | Explanation | Number of swimmer | | |
|---|---|---|---|---|
| | | Study 1 | Study 2 | Overall |
| A Elite | Competitive swimming; >3 training sessions a week | 3 | 4 | 7 |
| B Recreational | Non-competitive, but regular training/workout | 2 | 6 | 8 |
| C Occasional | No regular training | 3 | 2 | 3 |

### 5.1. Swim performance evaluation

For the evaluation of the automatic performance measurement, we accomplished a 7 × 50 m *Stroke Efficiency Test* according to the protocol described by Maw and Volkers [25]. Eight swimmers have taken part in this study.

Each of the eight participants swam one lane seven times in crawl technique on a 2 min cycle with increasing or decreasing speed. Beside the wrist acceleration, we measured manually the needed time intervals to compute $\bar{v}$ and *DPS* with a stopwatch. In addition to the stop watch times, another experimenter labeled start and end of a lane, pass of 5 and 45 m point, as well as all strokes. For the second manual labeling, we used a hand-held PC running the CRN Toolbox [26]. In total, we recorded acceleration data of 56 lanes together with two manual time stamps of the stopwatch and the labeling device.

For comparison, we first evaluated the accuracy of the manual time measurements. The two independent manual annotations allowed us to evaluate the manual annotation variation. In our study, the two manual measurements revealed an error with a standard deviation of ±0.2 s per time event (start, stop, and arm stroke). The manual time measurement error is due to human reaction times and variations in human event identification. It introduces a significant error on the *TPS* measurement. For a high swimming velocity of 100 m/min and a low *TPS* of 1 s, the upper bound error is ±1.33% for the velocity and ±13.3% for the *TPS*.

To assess the reliability of the automatic parameter extraction algorithm we compared the positions of the detected events to the mean timings of the manual annotations. The start and stop events have all been detected correctly by our automatic detection algorithm. The deviation from the expected position is in the range of ±0.3 s for the pool-start and ±0.2 s for the wall-strike. The strokes are detected reliably except for the first or last stroke in one lane, which are occasionally missed. This is not critical, as this does not affect our *TPS* calculation. The maximum error of the detected stroke events from the expected positions is in the range of ±10% of the *TPS*. This deviation depends mainly on the swimmer's style and the swimming speed as this influences the width of the peak. The time measurement errors of the automatic event detection have the following influence on the velocity and the *TPS* calculation: For a high velocity of 100 m/min and a small number of 15 strokes per lane, the upper bound error is 1.67% for the velocity and 1.33% for the *TPS*.

While the manual velocity measurement is slightly more accurate than the automatic one, the automatic *TPS* extraction clearly outperforms the manual measurement. However, ideally only the 40 m mid-pool part is used to determine the velocity, which is not measurable from the acceleration data. Therefore, the velocity calculation in the automatic method is based on the whole 50 m lane. This slightly affects the absolute velocity value, because swimmers have a higher velocity during the first 5 m of the lane due to the wall push-off.

The *Stroke Efficiency* graphs of the four best performing swimmers are plotted in Fig. 13(a). The *Stroke Efficiency* graphs of the four less experienced swimmers are depicted in Fig. 13(b). The small numbers beside the markers on the graph indicate the order in which the lanes were swum. One can see that the better swimmers cover a wider range of 27–41 m/min swimming speed difference between the slowest and fastest performance compared to the less skilled swimmers, who only have 12–19 m/min swimming speed difference between the slowest and fastest performance. Secondly, the better swimmers have an approximate linear performance, slightly falling with increasing speed. A decreasing *DPS* with increasing velocity is expected due to an increased *slippage*, which results in an increasing number of strokes per lane. The less skilled swimmers do not have this characteristic curve of the good swimmers. Three of them could not control their swimming velocity properly, resulting in a nonlinear curve jumping between slower and faster swimming velocities. In addition, the performance decreases with increasing number of lanes swum. The performance moves towards the origin regardless of whether the speed is increased or decreased. Exhaustion is the explanation for this observation. The non-experienced swimmers became tired with increasing number of lanes swum, resulting in a control loss of their swimming technique.

### 5.2. Swim technique evaluation

For the validation of body-balance and body-rotation measurement, twelve subjects swam five pool lanes. They swum the first lane with normal leg kicks and a good body balance. The second lane they swum with very weak leg kicks to provoke a bad body balance. The third to fifth lane they swum with their normal body rotation, with minimal body rotation (ideally $\gamma = 0°$), and with as much body rotation as possible (ideally $\gamma = 90°$).

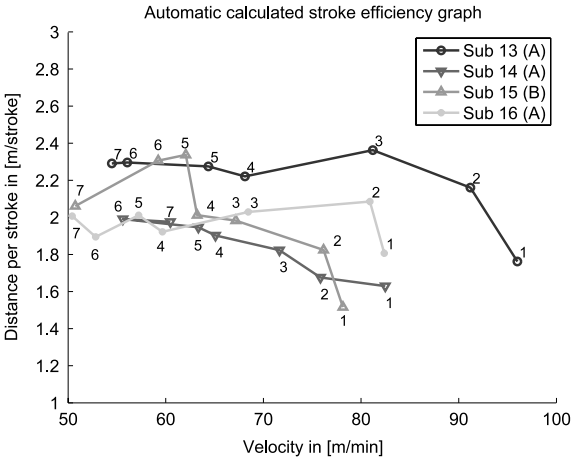


(a) Swim Technique Analysis Graphs of the four best swimmers.

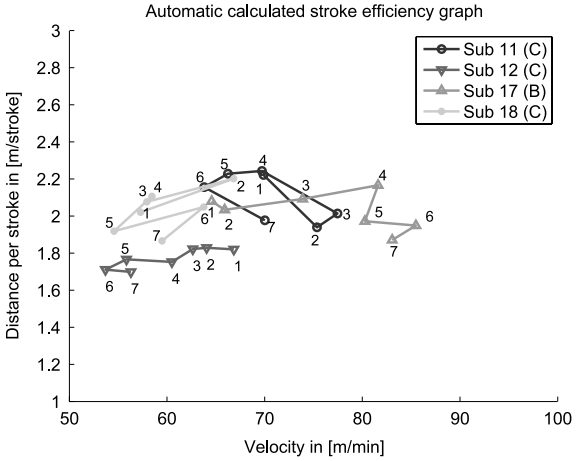


(b) Swim Technique Analysis Graphs of the four less experienced swimmers.

**Fig. 13.** Swim Technique Analysis Graphs measured automatically.

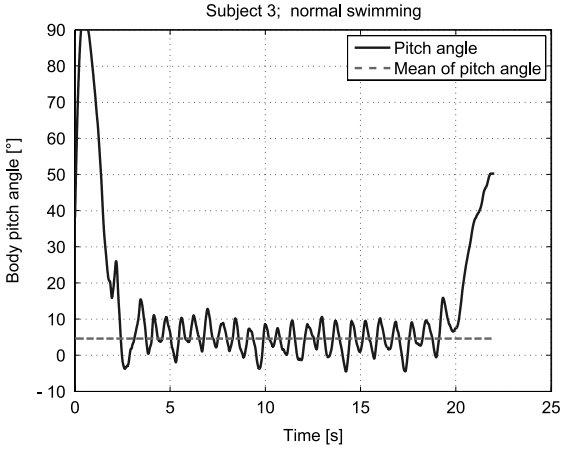


**Fig. 14.** Example of the pitch angle during one line.

### 5.2.1. Body balance evaluation

In Fig. 14, the pitch angle of one swimmer is plotted for one complete lane. As explained in Section 4.2.3 the pitch angle measurement is strongly influenced by the forward swim acceleration and deceleration. This results in a sinusoidal oscillation around the pitch angle. The dashed line in Fig. 14 is the mean pitch angle of the mid-pool part. One can see that this swimmer has an average pitch angle of 5°.

Overall, the twelve swimmers had an average pitch angle $\beta_{normal}$ of 5.2° with a *standard deviation* (SD) of 4.2° for the first lane where they were swimming with their normal leg kicks. For their second lane with only reduced leg kicks the twelve swimmers had an average pitch angle $\beta_{bad}$ of 12.1° with a SD of 4.3°. In Fig. 15 we have plotted the difference angle $\Delta\beta = \beta_{bad} - \beta_{normal}$. One can see that $\beta_{bad}$ is always bigger than $\beta_{normal}$ ($\Delta\beta > 0$) for each subject. However, not all swimmers could control their body balance similarly well. This corresponds to our observation during the experiment.

During the data recordings, a human observer estimated the body balance of each swimmer. The comparison of these human estimations with the measured angles confirmed that an angle estimation by an observer is very difficult from outside the pool and is unusable, at least if an untrained person is observing and estimating the body balance.

### 5.2.2. Body rotation evaluation

From the continuous rotation angle measurement, we extracted the following parameters for each lane:

- The average amplitude $\bar{A}_{roll}$ of all roll angles of upper and lower body part:

$$\bar{A}_{roll} = \frac{1}{N} \cdot \sum_{n=1}^{N} \frac{A_{Un} + A_{Ln}}{2}. \tag{3}$$

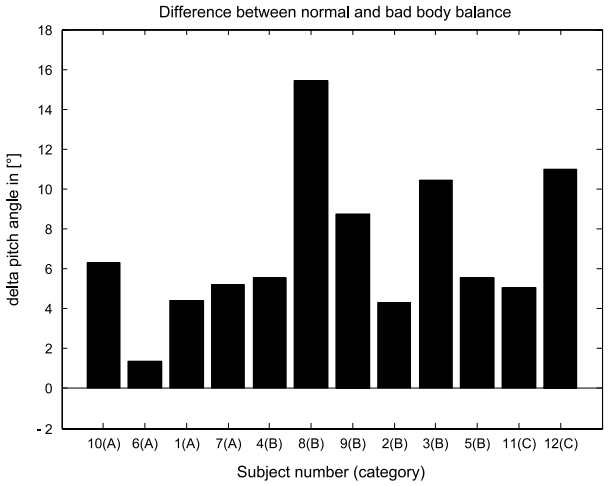


**Fig. 15.** Difference in pitch angles between good and bad body balance of all twelve subjects.

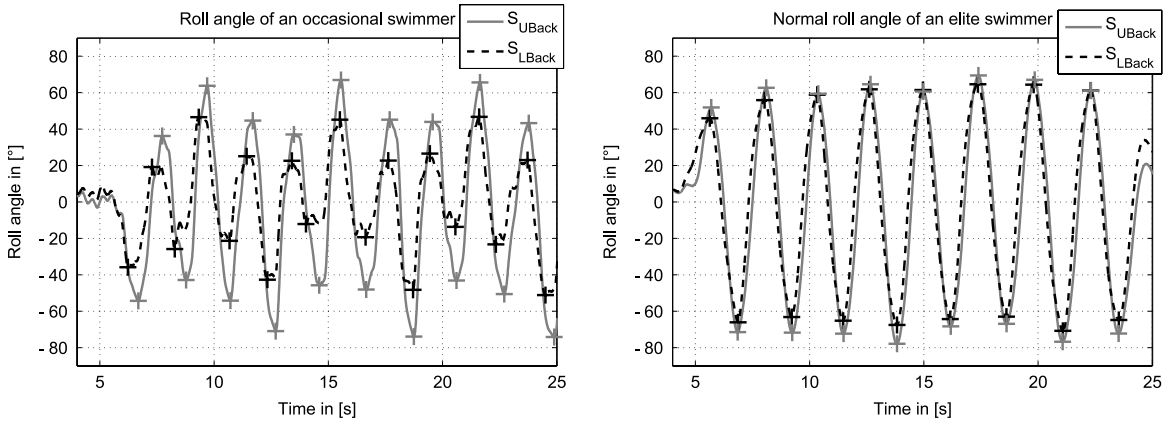


(a) Roll angle of an occasional swimmer.

(b) Roll angle of an elite swimmer.

**Fig. 16.** Roll angle of (a) an occasional and (b) an elite swimmer.

- The average difference between roll angle amplitude of upper and lower body part:

$$\Delta\bar{A}_{roll} = \frac{1}{N} \cdot \sum_{n=1}^{N} |A_{Un} - A_{Ln}|. \tag{4}$$

- The average time shift between amplitude peaks of upper and lower body part:

$$\Delta\bar{t}_{roll} = \frac{1}{N} \cdot \sum_{n=1}^{N} t_{AUn} - t_{ALn} \tag{5}$$

with

- $N$ number of arm strokes.
- $A_{Un}$ the $n$th roll amplitude of the upper body part.
- $A_{Ln}$ the $n$th roll amplitude of the lower body part.
- $t_{AUn}$ the $n$th time point of the upper body roll amplitude.
- $t_{ALn}$ the $n$th time point of the lower body roll amplitude.

The body rotation of two different swimmers is shown in Fig. 16. The data in Fig. 16(a) belongs to an occasional swimmer and the one in Fig. 16(b) to an elite swimmer. The body rotation of lower and upper back are drawn separately. One can see that the body rotation amplitudes of the elite swimmer are larger than the body rotation amplitudes of the less experienced swimmer. The rotation of lower and upper back is almost the same for the elite swimmer whereas there are big variations in the rotation amplitudes of upper and lower back for the occasional swimmer. Finally, there is a time shift between the

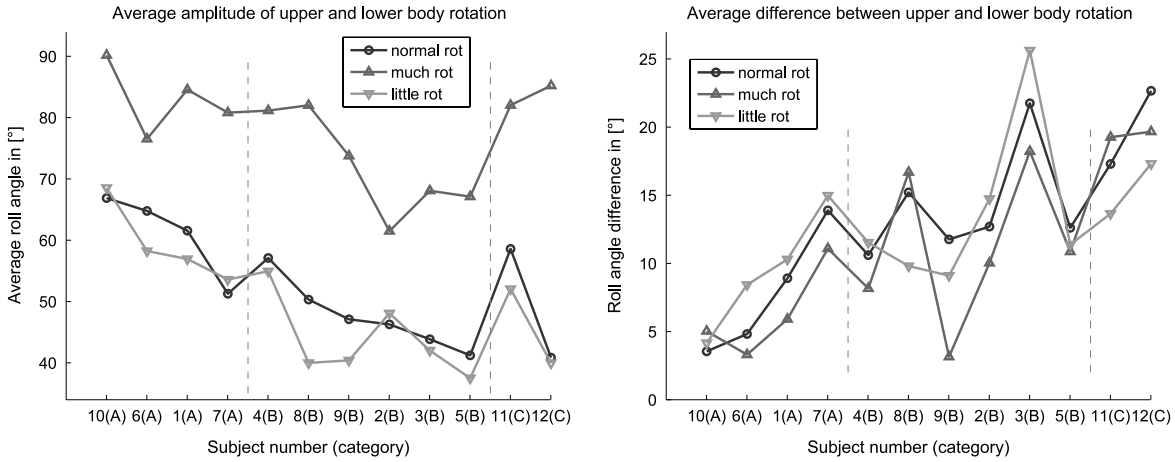


(a) Average amplitude $\bar{A}_{roll}$ of upper and lower body rotation.

(b) Average difference $\Delta\bar{A}_{roll}$ between upper and lower body rotation.

**Fig. 17.** Summary of the body rotation evaluation study.

**Table 2**
Summary of roll amplitudes $\bar{A}_{roll}$, roll amplitude differences $\Delta\bar{A}_{roll}$ and time shifts $\Delta\bar{t}_{roll}$ between lower and upper back rotation of swimmers within the three swim categories.

| Cat. | $\bar{A}_{roll} \pm$ SD | $\Delta\bar{A}_{roll} \pm$ SD | $\Delta\bar{t}_{roll} \pm$ SD |
|---|---|---|---|
| A | $61.1° \pm 6.9°$ | $7.8° \pm 4.7°$ | $79\ \text{ms} \pm 65\ \text{ms}$ |
| B | $47.6° \pm 5.5°$ | $14.1° \pm 4.0°$ | $127\ \text{ms} \pm 63\ \text{ms}$ |
| C | $49.7° \pm 12.5°$ | $20.0° \pm 3.8°$ | $140\ \text{ms} \pm 15\ \text{ms}$ |

maximum of lower and upper back rotation amplitudes for the occasional swimmer, which is not the case for the elite swimmer.

In Fig. 17(a) we plotted the average roll amplitude for each of the three lanes of all twelve subjects. Our experiment showed that the subjects struggled to swim with little body rotation. We explain this fact by the natural shoulder movement when doing the crawl strokes, where some amount of body rotation is almost inevitable. In Fig. 17(b) we plotted the average difference between upper and lower body for all three lanes and all subjects. The torsion is very similar for all three lanes within one subject; however, the torsion differs among the subjects with a tendency to increasing torsion for less experienced swimmers.

Comparing the above explained parameters between the three swimmer categories leads to the results in Table 2. For these values, the first lane of normal swimming of every swimmer was taken into account. These results confirm the observations discussed previously. Elite swimmers rotate noticeably more compared to recreational or occasional swimmers. Elite swimmers are able to swim more constantly, resulting in a smaller variance of roll amplitudes. They rotate their whole body avoiding skewing of the body, which can be seen by the smaller difference between the rotation of the lower and upper back. Finally, the average time shift between the rotation of upper and lower back is smaller for better swimmers, which is a measure of the synchronization of the body rotation.

Whereas these facts are already known beforehand, main result of our experiment is the verification that we are able to measure these small, but important differences between good and less experienced swimmers.

Similarly as for the body balance, we compared the body rotation angle measurement of the sensors with the observer's estimation. Whereas the human observer has estimated the angles around 80° very well, he underestimated the angles for small angles by up to 20°.

## 6. Conclusion and outlook

We built a system for swimming performance and technique analysis. We developed algorithms to extract important parameters for swimming such as swim velocity, arm strokes, distance per arm stroke, body balance, and body rotation. We developed a *SwimModel* for a detailed analysis of the measured body acceleration and an evaluation of our body-rotation and body-balance measurement. Validation of the sensor angle measurement showed that we can measure the roll angle accurately with our method. With studies on 18 swimmers we showed that our system can extract the above explained swim parameters. The results of the stroke efficiency evaluation are consistent with the visual observations. The averaged body balance measurement allows differentiation between a good and bad body balance. The longitudinal body rotation measurement can be used to quantify a swimmer's body-rotation technique by analyzing absolute rotation amplitudes and

comparing the amplitudes of the upper and lower body. To our knowledge, this is the first time that a body worn system was used to perform a stroke efficiency evaluation and measure body-balance and body-rotation.

Our evaluation methods open new possibilities for state of the art swimming training, as objective values can be provided at all times for the complete training. Many parameters are hard to judge from the trainer's position outside the pool. Therefore, such a wearable system provides the possibility to continuously monitor and evaluate parameters that can otherwise only be extracted occasionally. This is advantageous for a swimming trainer who has to set up the best training plan for his swimmers.

So far, the data analysis is based on off-line algorithms. The swim data is evaluated with a personal computer after the swimming exercise. Since the algorithms do not require a global view on the data, this allows for an online algorithm implementation. Roggen et al. have shown that computations similar in complexity to those carried out in this work are suited for online implementation in miniature sensor nodes of the size of a button [27].

With an online algorithm, a swimmer can directly benefit from the wearable system through the online feedback device. The feedback is especially valuable if a swimmer wants to work on specific problems, like his body-balance or body-rotation, as he can get continuous feedback on his actual performance and react accordingly. To make the *SwimMaster* system applicable in everyday swim training, we envision a swimsuit with integrated sensors and feedback capabilities. In combination with an online swim-parameter extraction algorithm, swimmers can benefit from the feedback to work on specific problems also when there is no trainer aside.

## Acknowledgments

The authors would like to thank the swimmers and trainers of the swim club Appenzell (SCAP) for taking part in the studies.

## References

[1] S. Tarpinian, The Triathlete's Guide to Swim Training, VeloPress, 2005.
[2] A.B. Craig, D.R. Pendergast, Relationships of stroke rate, distance per stroke, and velocity in competitive swimming, Medicine and Science in Sports 11 (3) (1979) 278–283.
[3] B. Auvinet, E. Gloria, G. Renault, E. Barrey, Runner's stride analysis: comparison of kinematic and kinetic analyses under field conditions, Science & Sports 2002 17 (2002) 92–94.
[4] F. Michahelles, B. Schiele, Sensing and monitoring professional skiers, IEEE Pervasive Computing 4 (3) (2005) 40–46.
[5] D. Spelmezan, J. Borchers, Real-Time Snowboard Training System, CHI '08 extended abstracts on Human factors in computing systems, April 05–10, 2008, Florence, Italy (doi:10.1145/1358628.1358852).
[6] T. Holleczek, C. Zysset, B. Arnrich, D. Roggen, G. Tröster, Towards an interactive snowboarding assistance system, in: Proceedings of the 13th IEEE International Symposium on Wearable Computers, ISWC 2009 vol. 2, IEEE, 2009, pp. 147–148.
[7] M. Estivalet, P. Brisson, The Engineering of Sport 7, Springer Paris, Paris, 2008, doi:10.1007/97-2-287-99056-4.
[8] H. Ghasemzadeh, V. Loseu, E. Guenterberg, R. Jafari, Sport training using body sensor networks: a statistical approach to measure wrist rotation for golf swing, in: The Fourth International Conference on Body Area Networks, BodyNets 09, Los Angeles, CA, April, Los Angeles, 2009.
[9] H. Ghasemzadeh, V. Loseu, R. Jafari, Wearable coach for sport training: a quantitative model to evaluate wrist-rotation in golf, Journal of Ambient Intelligence Smart Environment 1 (2) (2009) 173–184. doi:10.3233/AIS-2009-0021.
[10] R. Anderson, A. Harrison, G.M. Lyons, Rowing, Sports Biomechanics 4 (2) (2005) 179–195. doi:10.1080/14763140508522862.
[11] M. Beetz, B. Kirchlechner, M. Lames, Computerized real-time analysis of football games, IEEE Pervasive Computing 4 (3) (2005) 33–39.
[12] M. Beetz, N.V. Hoyningen-Huene, J. Bandouch, B. Kirchlechner, S. Gedikli, A. Maldonado, Camera-Based Observation of Football Games for Analyzing Multi-Agent Activities, ACM Press, NY, New York, USA, 2006, doi:10.1145/1160633.1160638.
[13] M. Lapinski, E. Berkson, T. Gill, M. Reinold, J.A. Paradiso, A Distributed Wearable, Wireless Sensor System for Evaluating Professional Baseball Pitchers and Batters, IEEE, Linz, 2009, doi:10.1109/ISWC.2009.27.
[14] J. Hey, S. Carter, Pervasive computing in sports training, Pervasive Computing, IEEE (2005) 54.
[15] Y. Ohgi, Microcomputer-based acceleration sensor device for sports biomechanics, Sensors 1 (2002) 699–704.
[16] N.P. Davey, An Accelerometer-Based System for Elite Athlete Swimming Performance Analysis, vol. 5649, SPIE, 2005, doi:10.1117/12.582264.
[17] D. James, N. Davey, T. Rice, An Accelerometer Based Sensor Platform for in-situ Elite Athlete Performance Analysis, vol. 3, IEEE, 2004, doi:10.1109/ICSENS.2004.1426439.
[18] R. Chan, Swimming lap counter, Patent US 20070293374, December 2007.
[19] S.E. Slawson, L.M. Justham, A.A. West, P.P. Conway, M.P. Caine, R. Harrison, Accelerometer profile recognition of swimming strokes, The Engineering of Sport 7 (2008) 81–87.
[20] A.J. Callaway, J.E. Cobb, I. Jones, A comparison of video and accelerometer based approaches applied to performance monitoring in swimming, International Journal of Sports Science & Coaching 4 (1) (2009) 139–153.
[21] M. Bächlin, K. Förster, J. Schumm, D. Breu, J. Germann, G. Tröster, An automatic parameter extraction method for the 7 × 50 m stroke efficiency test, in: Proc. of the 3rd International Conference on Pervasive Computing and Applications, 2008, pp. 442–447.
[22] M. Bächlin, K. Förster, G. Tröster, SwimMaster, ACM Press, New York, New York, USA, 2009, doi:10.1145/1620545.1620578.
[23] M. Bächlin, G. Tröster, Pervasive computing in swimming: a model describing acceleration data of body worn sensors in crawl swimming, in: Proceedings of the 4th International Conference on Pervasive Computing and Applications 2009, 2009.
[24] K. Förster, M. Bächlin, G. Tröster, Non-interrupting user interfaces for electronic body-worn swim devices, in: Proceedings of the 2nd International Conference on Pervasive Technologies Related to Assistive Environments, ACM, 2009.
[25] G.J. Maw, S. Volkers, Measurement and application of stroke dynamics during training in your own pool, Australian Swim. Coach 12 (3) (1996) 34–38.
[26] D. Bannach, K. Kunze, P. Lukowicz, O. Amft, Architecture of Computing Systems — ARCS 2006, in: Lecture Notes in Computer Science, vol. 3894, Springer, Berlin, Heidelberg, Berlin, Heidelberg, 2006, doi:10.1007/11682127.
[27] D. Roggen, N.B. Bharatula, G. Tröster, M. Stäger, P. Lukowicz, From sensors to miniature networked sensor buttons, in: Proc. of the 3rd Int. Conf. on Networked Sensing Systems, INSS06, 2006, pp. 119–122.